Scientific Research Publishing

Journal of Sensor Technology, 2024, 14, 35-50
https://www.scirp.org/journal/jst
ISSN Online: 2161-1238
ISSN Print: 2161-122X

A Glassy Carbon Electrode Modified with Cellulose Nanofibrils from *Ammophila arenaria* for the Sensitive Detection of L-Trytophan

Sondes Bourigua[1], Feriel Boussema[1], Zayneb Jebali[1], Houcine Barhoumi[1], Hatem Majdoub[1], Abderrazak Maaref[1], Nicole Jaffrezic-Renault[2*]

[1]Laboratory of Advanced Materials and Interfaces, Faculty of Sciences, University of Monastir, Monastir, Tunisia
[2]Institute of Analytical Sciences, University of Lyon, Villeurbanne, France
Email: *nicole.jaffrezic@univ-lyon1.fr

How to cite this paper: Bourigua, S., Boussema, F., Jebali, Z., Barhoumi, H., Majdoub, H., Maaref, A. and Jaffrezic-Renault, N. (2024) A Glassy Carbon Electrode Modified with Cellulose Nanofibrils from Ammophila arenaria for the Sensitive Detection of L-Trytophan. *Journal of Sensor Technology*, **14**, 35-50.
https://doi.org/10.4236/jst.2024.143003

Received: August 5, 2024
Accepted: September 21, 2024
Published: September 24, 2024

Abstract

L-tryptophan is an essential amino acid for human health. Nanofibrillated cellulose (NFC) from marram grass (*Ammophila arenaria*) extracted from plants harvested in the center of Tunisia was used for the first time for the modification of a glassy carbon electrode (GCE), for the sensitive detection of L-tryptophan (Trp). After spectroscopic and morphological characterization of the extracted NFC, the GC electrode modification was monitored through cyclic voltammetry. The NFC-modified electrode exhibited good analytical performance in detecting Trp with a wide linear range between 7.5×10^{-4} mM and 10^{-2} mM, a detection limit of 0.2 μM, and a high sensitivity of 140.0 $\mu A \cdot mM^{-1}$. Additionally, the NFC/GCE showed a good reproducibility, good selectivity versus other amino acids, uric acid, ascorbic acid, and good applicability to the detection of Trp in urine samples.

Keywords

Nanofibrillated Cellulose, Chitosan, Chemically Modified Glassy Carbon Electrode, Electrochemical Detection, L-Tryptophan

1. Introduction

The detection of amino acids is important in different fields of research: medicine, food, biotechnology, and wine industries. L-Tryptophan (Trp) whose standard chemical name is (2S)-2-amino-3-(1H-indol-3-yl) propanoic acid and the molecu-

lar formula is $C_{11}H_{12}N_2O_2$ (molecular weight: 204.22 g/mole), is an essential amino acid with biochemical, nutritional, and medical significance for humans [1]. It is important for normal growth in infants and nitrogen balance in adults [2]. L-tryptophan (Trp) is considered a "necessary" amino acid since the body cannot produce it on its own [3], it can only be obtained through food or supplementation. Trp is present in a wide variety of protein-containing foods such as milk, egg, poultry, cheese, nuts, bananas, and fish [4]. It is a precursor for niacin, melatonin, and serotonin, these molecules being involved in regulating mood [5]. Consequently, it has been reported that abnormal levels of Tryptophan may cause several serious diseases including delusions and hallucinations [6]. Furthermore, taking an overdose of tryptophan induces dizziness, drowsiness, loss of appetite, nausea, and hepatic disease [4]. The World Health Organization (WHO) suggests daily consumption of 4 mg/kg of body weight of Trp [4]. Trp is also a biomarker of certain diseases; lower concentrations of Trp were observed in plasma from patients with Alzheimer's disease [7], with colorectal and prostate cancer [8]. Hence, the sensitive and selective determination of tryptophan is essential in medicine and food products. Different analytical techniques are used to determine Trp, including high-pressure liquid chromatography [9], chemiluminescence [10], capillary electrophoresis [11], and spectroscopic detection [12]. Still, they require complicated and expensive equipment, multi-step sample treatment, and are time-consuming. As tryptophan is electroactive, a highly sensitive, selective, simple, low cost and quick-responding electrochemical method would gain more attention.

However, it is still difficult to measure tryptophan directly at unmodified electrodes due to the slowness of the redox process which leads to high overpotential at the electrode [13] [14]. Therefore, fabricating modified electrodes using highly conductive and catalytic materials is very important to reduce the overpotential and enhance the electrochemical response. For the electrochemical detection of Trp, different kinds of synthesized nanomaterials were used to modify the electrodes including metal/metal oxide nanoparticles, conductive polymers, and carbon-based nanomaterials [15].

Because of the availability of natural polymers and their numerous qualities: biocompatible, biodegradable, low cost, and nontoxic, they have been used in various formulations [16]. Different polysaccharides have been used to modify electrodes such as cellulose [17], alginate [18], chitin [19], chitosan [20] and pectin [21].

Cellulose is the major component—around 35% - 50%—in the lignocellulosic biomass, mainly localized in the plant cell wall. It is composed of the linear homopolysaccharide of b-1,4-linked anhydro-D-glucose units. In cellulose fibers, there are some crystalline parts where the chain molecules are orderly packed, called nanofibrils. Recently, nanofibrillated cellulose has gained attention in both research and industrial areas, due to its attractive properties, such as excellent mechanical properties, high surface area, high density of hydroxyl groups for modi-

fication properties, ionic conductivity, transparency, with 100% environmental friendliness. Nanocellulose is a natural nanomaterial that can be extracted from the plant cell wall [22]. It exists in a quasi-pure state in the form of cotton seed hair, but most often is found combined with other polysaccharides. The nanofibrillated cellulose (NFC) was produced by mechanically treating cellulose suspensions through high-pressure homogenizers. The typical cross-section of nanofibrils ranges from 4 to 20 nm depending on their origin [23] [24]. NFC has been used for the modification of carbonaceous electrodes, for the sensitive electrochemical detection of metal ions [25], and of atrazine [26]. A NFC/RGO nanocomposite has been used for the electrochemical detection of fenitrothion organophosphorus pesticide [27] and for the detection of p-nitrophenol [28].

In this work, the NFC-modified glassy carbon electrode (GCE) was built and used for the electrochemical detection of tryptophan, for the first time. The modification of the GCE was carried out with the encapsulation of NFC in a chitosan (CS) film for higher stability and greater detection sensitivity. The electron transfer during the redox reaction of Trp on the CS/NFC-modified GCE was characterized. After the analytical performance of the CS/NFC-modified GCE was determined, it was applied to the detection of Trp in real urine samples.

2. Experimental

2.1. Chemicals and Reagents

$K_4Fe(CN)_6{\cdot}3H_2O$, $K_3Fe(CN)_6$, KCl, L-tryptophan, uric acid, ascorbic acid, and chitosan were purchased from Fluka Chemika. TEMPO (2,2,6,6,-tetramethylpiperidine 1-pxyl) was purchased from Sigma-Aldrich. The buffer solution used for all experiments was phosphate buffer saline (PBS) containing 137 mM NaCl, 2.7 mM KCl, 0.01 M KH_2PO_4 and 0.01 M K_2HPO_4, pH 7. All solutions were prepared in ultrapure water (resistance 18.2 MW·cm^{-1}) produced by a Millipore Milli-Q system. The NFC material was extracted from marram grass (*Ammophila arenaria*) collected in the central western area of Tunisia (Gafsa).

2.2. Instrumentation

Fourier transform infrared (FTIR) spectra (from 4000 to 400 cm^{-1}) were obtained using a BX FTIR system spectrometer, Perkin Elmer Company, Waltham, MA, USA. KBr pellets technique was used for sample preparation.

The transmission electron microscope (TEM) image of the extracted NFCs was taken using a Jeol 200 CX transmission electron microscope at 80 kV. About 0.5 μL of diluted suspension of NFC (about 0.1%) was deposited onto a 300 mesh carbon-coated grid.

X-ray diffraction (XRD) patterns were collected by a Bruker diffractometer (D8 Advance, Germany) with Cu-Kα radiation (λ = 0.1548 nm).

Electrochemical experiments were carried out using an Autolab (PGSTAT 302 N, Eco Chemie). All measurements were performed in a dark Faraday cage at

room temperature. A conventional three-electrode system consisting of a platinum counter-electrode, an Ag/AgCl/KCl as the reference electrode, and a glassy carbon electrode (GCE, f 3 mm) as the working electrode was used. Differential Pulse Voltammetric (DPV) measurements were carried out at a scan rate of 50 mV/s with an accumulation time of 20 s.

2.3. Production of NFC

By a conventional soda-pulling process and bleaching treatment, the cellulose fibers were extracted from Marram grass, then the fibers were treated by TEMPO-mediated oxidation to generate carboxyl groups. Oxidation was carried out at pH 10 following the previously reported method (Jebali *et al.*, 2018). Briefly, 5 g of fibers were dispersed in 500 mL sodium phosphate buffer (0.05 mol·L^{-1}, pH 7) containing 25 mg of TEMPO and 250 mg of NaBr. Then 1.13 g of NaCl (80%) and 2 mol·L^{-1} of NaClO were added to the flask in one step and the suspension was left under magnetic stirring at 60˚C for 6 h. At the end of the oxidation reaction, 100 mL of ethanol was added and the obtained modified fibers were filtered. This operation was carried out several times with water to remove any salt. Then a suspension of 1.5 wt% of prepared fibers was homogenized in a high-pressure homogenizer from GEA (NS 1001 L PANDA 2 K-GEA, Italy). After six shear cycles (3 × 30 bar; 3 × 600 bar), a thick transparent NFC-COO$^-$ gel was obtained [24].

2.4. Functionalization of the Glassy Carbon Electrode

Before the electrode modification, the bare glassy carbon electrode (GCE) was polished with 0.5 µm alumina solution. The GCE was then fully rinsed with water and sonicated in ethanol and deionized water for 3 min. Next, the GCE was scanned in 0.5 M H_2SO_4, at 50 mV/s for many cycles between −0.2 V and 1.3 V.

Subsequently, 5 µL of CS (the optimized concentration, 1 mg/mL) solution was deposited on the GCE, then 5 µL of NFC (optimized concentration: 1 mg/mL) was deposited on the CS/GCE. The obtained CS/NFC modified surface was dried for 24 hrs at room temperature.

3. Results and Discussion

3.1. FTIR Characterization of NFC

The Fourier transform-infrared spectroscopy (FTIR) spectrum of NFC is illustrated in **Figure 1** and shows distinct absorption bands. The bands located at 3330 cm^{-1} were attributed to O–H stretching vibration. The band at 2906 cm^{-1} was assigned to the aliphatic C–H -stretching vibration and the band at 1660 cm^{-1} associated with the O–H bending vibration of absorbed water. CNF showed a band at 1614 cm^{-1}, which was likely due to the introduction of carboxylic groups into the primary alcohol groups on the surface of cellulose nanofibrils after TEMPO mediated oxidation. The characteristic bands of the glucosic ring appear in the 1000 - 1162 cm^{-1} region.

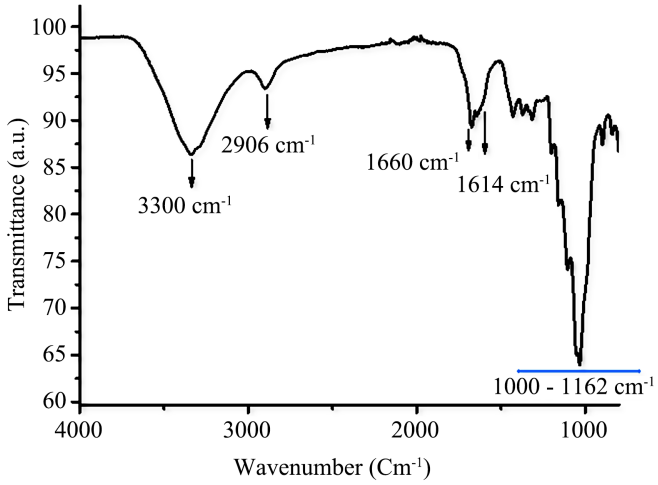

Figure 1. The Fourier transform-infrared spectroscopy (FTIR) spectrum of NFC.

3.2. Morphological Characterization of NFC

The morphological features of CNF were assessed by TEM observation (**Figure 2(a)**). Nanosized fibrils with a width distribution centered around 3 - 6 nm are observed which is a good indication that the individual fibrils correspond to elementary cellulose fibrils composed of altered amorphous and crystalline domains. The crystalline structure of NFC was confirmed through X-ray diffraction (**Figure 2(b)**); a strong peak is observed at 18˚ corresponding to the 002 plane [26].

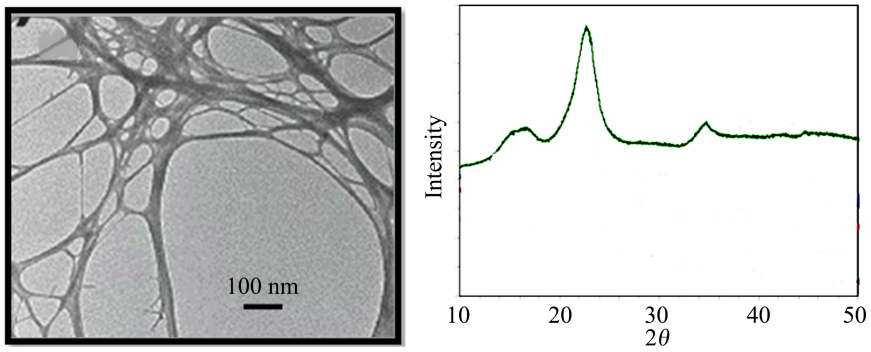

Figure 2. (a) TEM observation of NFC; (b) XRD spectrum of NFC.

3.3. Electrochemical Characterization of NFC/CS Modified GCE

The electrochemical behavior of the different modified electrodes was examined by cyclic voltammetry (CV). As shown in **Figure 3**, a pair of reversible and well-defined redox peaks was observed on the bare GCE, with a ΔEp of 100 mV and an intensity ratio of about 1:1 between anodic and cathodic peak currents demonstrating that the glassy carbon electrode (GCE) has a quasi-reversible electrochemical reaction with the $[Fe(CN)_6]^{3-/4-}$ couple [26]. The redox currents decreased significantly after the GCE was modified with CS/NFC, proving the electrode modification.

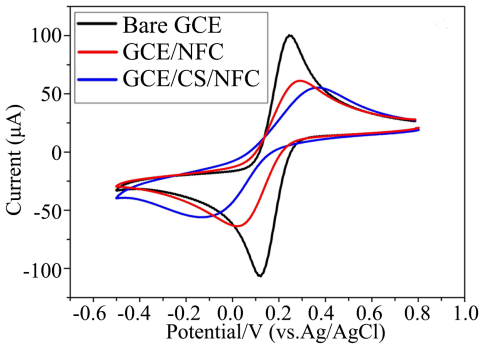

Figure 3. Cyclic voltammograms of modified and unmodified GCE with NFC and CS in 0.1 M KCl solution containing 5 mM $[Fe(CN)_6]^{3-/4-}$ at scan rate of 50 mV·s^{-1}.

So, with the integration of NFCs and CS, the synergistic effect then took place at this electrochemical platform, leading to increased adsorption of electrochemically active sites, and of the effective electrode area.

3.4. Electrochemical Behaviour of L-Tryptophan

To determine the electrochemical behavior of 0.1 mM Trp in phosphate buffer solution (pH 7.0) on a GCE, CS/GCE, NFC/GCE, and a CS/NFC/GCE, cyclic voltammetry was investigated. From the electrochemical results shown in **Figure 4(a)**, it can be seen that Trp presents only one oxidation peak. No reduction peak was observed in the reverse scan, confirming that the electrochemical reaction is an irreversible process, in agreement with previous results [29]. As can be seen from **Figure 4(a)**, the oxidation peak at the bare GCE appears at 0.75 V, while at the CS/NFC/GCE the peak potential shifted negatively to 0.55 V and the peak current increased significantly. This observation proves that CS/NFC film can catalyze the oxidation of L-Tryptophan. The strong electrostatic attraction between CNF-COO^- (negatively charged) (pie < 2.8) and Trp molecule (pie = 5.89) can explain the increase in intensity. The conductive properties of NFC (2 mS/cm [30]) explain its role in favoring charge transfer. The DPV peaks presented in **Figure 4(b)** confirm the results obtained by cyclic voltammetry.

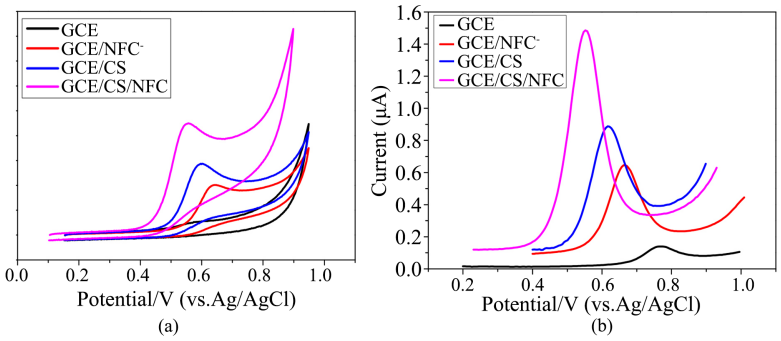

Figure 4. CVs of 0.1 mM of L-Tryptophan on a GCE and a CS/NFCs/GCE at scan rate of 50 mV·s^{-1} (0.01 M phosphate buffer solution (pH 7.0)) (a) and DPV of 0.1 mM of L-Tryptophan on a GCE and CS/NFCs/GCE at 50 mV·s^{-1} (0.01 M phosphate buffer solution (pH 7.0)) (b).

3.5. Optimization of the Experimental Conditions for Electrochemical Detection

3.5.1. Effect of pH Value

By increasing the buffer solution pH from 4.5 to 8.5, the anodic potential gradually decreased which confirms the direct participation of protons in the oxidation reaction of Trp at the CS/NFC/GCE. The anodic peak potential varies linearly with pH value, following this equation:

$$\text{Epa} = -55.43\text{pH} + 0.98, \quad R^2 = 0.996 \tag{1}$$

The slope (−55.43 mV/pH) is very close to the theoretical value of 59 mV/pH, showing an equal number of exchanged electrons and protons during the oxidation process.

The peak current response of Tryp varied also with the change of pH and the maximum peak current is at pH 7.0 (Figure 5); for pH higher than 7 the attractivity between Trp (pie 5.89) and NFC decreases. Subsequently, pH 7.0 was considered as the optimal electrolyte solution for the determination of L-Trp.

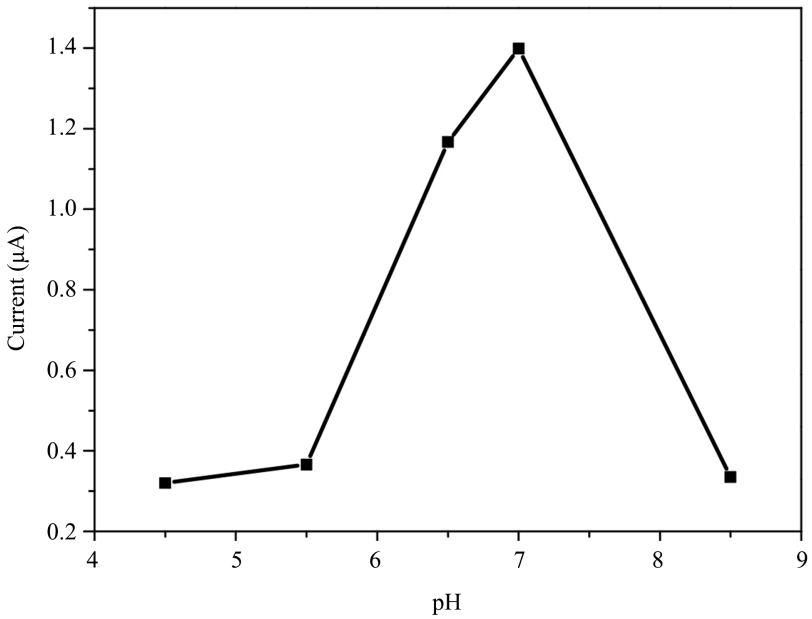

Figure 5. Effect of pH on peak current of 0.1 mM of L-Tryptophan at CS/NFCs/GCE (0.01 M phosphate buffer solution (pH 7.0)).

3.5.2. Effect of Scan Rate

CVs of 0.1 mM L-Trp at the CS/NFC/GCE, with various scan rates (20 to 500 $\text{mV}\cdot\text{s}^{-1}$) were investigated. As shown in Figure 6, the oxidation peak current for L-Tryptophan increases as the scan rate increases, suggesting that the electrocatalytic oxidation of L-Tryptophan at the CS/NFC modified GCE was a typical adsorption-controlled process. The linear relation between the oxidation peak intensity and the scan rate is the following one:

$$\text{Ipa}(\mu\text{A}) = 2.19 + 0.011v\left(\text{mV}\cdot\text{s}^{-1}\right), \quad R^2 = 0.991 \tag{2}$$

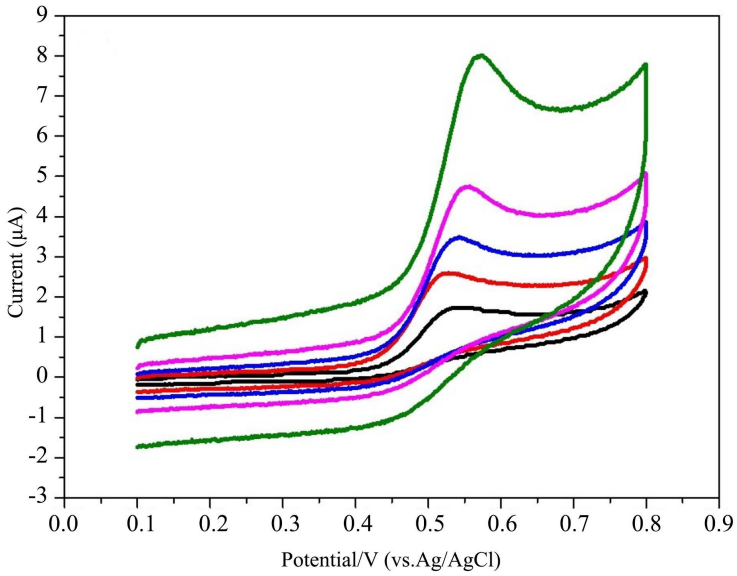

Figure 6. Effect of scan rate: overlay of cyclic voltammogram for oxidation of L-Trp at different scan rates.

In addition, the oxidation peak potentials shift positively as the scan rate increases. So, 50 mV/s is employed as the optimal scan rate in the following experiments. The plot of peak current vs. square root of scan rate ($v^{1/2}$) is linear over the whole studied range of scan rate, indicating that the electro-oxidation of Trp at the CS/NFC/GCE was a typical diffusion-controlled process, and the equation can be expressed as:

$$\mathrm{Ipa}\left(\mu\mathrm{A}\right) = 0.35v^{1/2} + 0.012,\ R^2 = 0.994 \tag{3}$$

Moreover, the relationship between log (ipa) and log of the scan rate was found to be linear.

$$\log \mathrm{ipa}\left(\mu\mathrm{A}\right) = 0.47 \log v - 0.39,\ R^2 = 0.990 \tag{4}$$

given a slope of 0.47 which is in agreement with the theoretical value of 0.5 for a diffusion-controlled process.

The number of electrons involved in the oxidation of tryptophan was calculated using the equation :

$$\mathrm{ipa} = nFQv/4RT \tag{5}$$

where ipa denotes the anodic peak current, Q denotes the amount of the integrated charge from the area of the voltammetric peak, F is the Faraday constant (96,500 C/mol), T denotes the temperature (298 K), R is the gas constant (8.314 J·mol^{-1}) and n is the number of transferred electrons. From the slope of ip versus v, the number of electrons transferred in the oxidation of L-Trp was calculated to be 1.66. Consequently, the oxidation process of L-Trp involves two electrons and two protons, and the oxidation reaction of Trp is irreversible.

The anodic peak potential (Epa) versus the logarithm of the scan rate ($\log v$) is a linear relationship:

$$\text{Epa} = 0.044 \log v + 0.54, \quad R^2 = 0.991 \tag{6}$$

Based on Laviron's relation [31], the linear plot of Epa versus $\log v$ reaches a slope of $(2.3RT/\alpha nF)$, which is equal to 0.044; the value of αn is calculated to be 1.34. According to Equation (7), the calculated α is 0.67.

$$\alpha = 47.7/(\text{Epa} - \text{Epa}/2) \tag{7}$$

where Epa and Epa/2 represent the formal potential and half of the formal potential value respectively.

3.6. Electrochemical Determination of L-Tryptophan

The electrochemical performance of Trp was investigated by Differential Pulse Voltammetry (DPV) on bare GCE and two modified electrodes: NFC/GCE and CS/NFC/GCE in PBS (pH 7.0) at 50 mV/s. **Figure 7(a)** displays the DPV signal for different concentrations of Trp at the bare GCE. The oxidation peak current was observed at 0.75 V. The peak current response of the electrochemical sensor presents a linear variation with the concentration of L-Tryptophan, over the range from 5×10^{-4} to 10^{-2} mM, with a sensitivity of 8.15 μA·mM^{-1}.

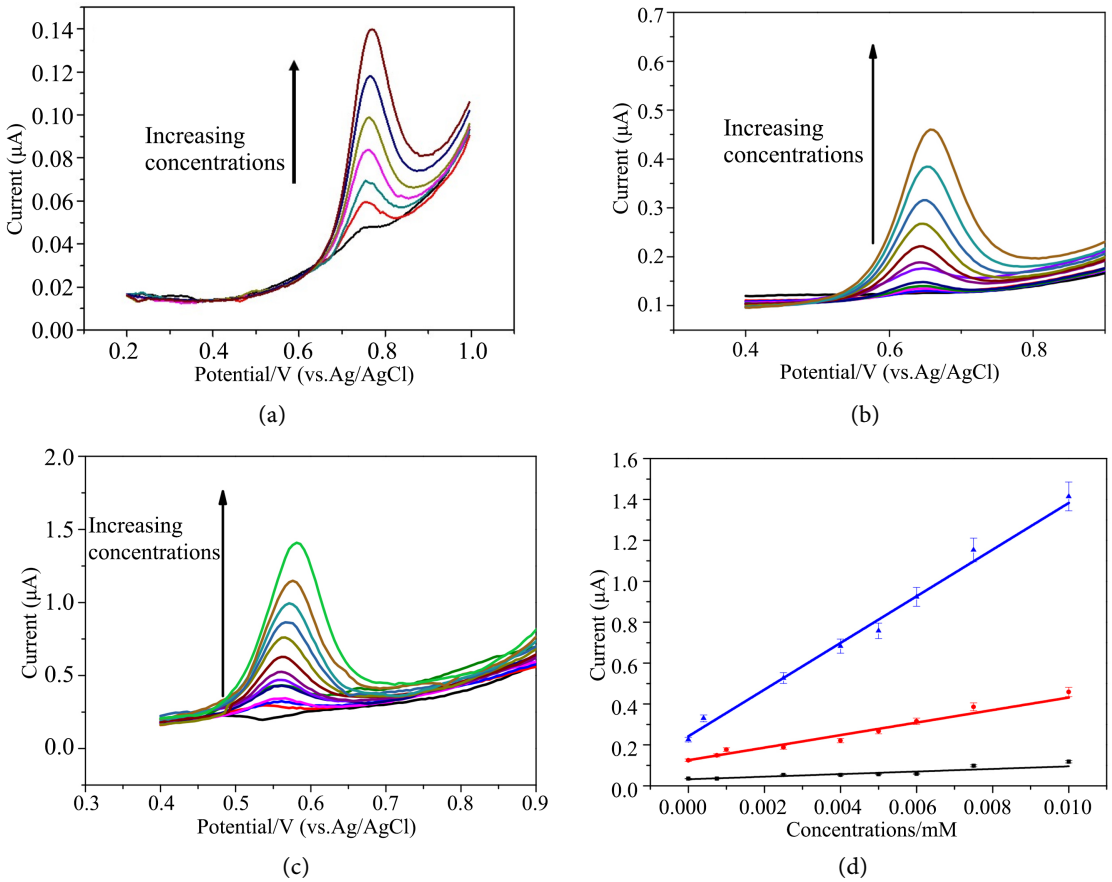

Figure 7. DPV detection of L-tryptophan in the concentration range from 7.5×10^{-4} to 10^{-2} mM, on bare GCE (a), on NFCs/GCE (b), on CS/NFCs/GCE (c) in 0.01 M phosphate buffer solution (pH 7.0), scan rate 50 mV/s and calibration curves of L-Tryptophan (d) at bare GCE (black line), at NFCs/GCE (red line) and at CS/NFCs/GCE (blue line). Experimental conditions: 0.01 M phosphate buffer solution (pH 7.0), scan rate 50 mV/s.

Figure 7(b) shows the DPV for different concentrations of Trp at the NFCs-modified GCE; The corresponding peak current at 0.64 V of L-Trp increases proportionally with the increase in concentration of L-Trp. The plot of the oxidation peak current versus concentration exhibits good linearity in the range of 7.5×10^{-4} mM to 10^{-2} mM with a sensitivity of 33.14 μA·mM^{-1}. A detection limit of 0.75 μM was obtained.

Figure 7(c) shows the DPV for different concentrations of Trp at the CS/NFCs modified GCE in the range of 4×10^{-4} mM to 10^{-2} mM; it was found that the anodic peak current shifts to the negative side and appeared at 0.55 V with an improved anodic peak response. The DPV curves clearly show that CS/NFC/GCE displays a proportionally increasing current response with increasing L-Trp concentration. The corresponding sensitivity of 140.0 μM·mM^{-1} is three times higher than the sensitivity of the NFC/GCE and a lower detection limit of 0.2 μM was obtained.

Figure 7(d) shows the plots of the L-Trp oxidation peak current versus L-Trp concentration on bare GCE, NFC/GCE, and CS/NFC/GCE. The excellent electrochemical sensing property was attributed to the CS/NFC film. The RSD on the measurements was 1%.

Furthermore, the analytical parameters of the proposed green nanocomposite CS/NFC were compared with the other modified electrodes, and the values are listed in Table 1. In comparison, our proposed sensor exhibits excellent electrocatalytic activity for the electrochemical determination of Trp: the lowest potential value was required for the Trp oxidation and the higher sensitivity was obtained.

Table 1. Comparison of CS/NFCs/GCE sensor with other reported electrochemical sensors for the determination of L-Tryptophan.

Modified Electrode	Potential	Limit of detection (μM)	Linear range (μM)	Sensitivity (μA/mM)	References
poly(L-Methionine)/3 Graph (a) (d)	0.76 vs. SCE	0.017	0.2 - 150	23.4	[32]
MnWO4 nanoplates encapsulated RGO nanocomposite (a) (d)	0.72 vs. Ag/AgCl	0.004	0.001 - 120	43.3	[3]
Poly(glycine) modified carbon nanotube paste electrode (b) (d)		0.42	20 - 100		[33]
Graphite electrode from waste batteries (c) (d)	0.75 V vs. SCE	1.73	5 - 150	32.4	[34]
Ni-ZIF-8/N S-CNTs/CS (a) (d)	0.72	0.69	5 - 850	12.2	[35]
Ta_2O_5-rGO (a) €	0.7 V vs. SCE	0.84	1-	-	[36]
3-neomenthylindene (b) (d)	0.79 V vs. Ag/AgCl		8 - 80	-	[37]
rGO-PTCA-chitosan (a) (d)	0.8 V vs. SCE	1.2	1000 - 10,000	62.19	[38]
MWCNTs-CTAB (a) (d) nanocomposite-modified	0.85 V vs. Ag/AgCl	1.6	4.9 - 64.1	-	[39]
Pectin (a)	0.65 V vs. Ag/AgCl	0.09	0.09 - 20	90.15	[21]
Chitosan/Nanofibrillated cellulose (a)	0.55 V vs. Ag/AgCl	0.2	0.75 - 100	111.36	This work

(a) GCE, (b) CPE, (c) graphite electrode, (d) DPV, (e) GC.

The stability of the modified electrode was studied by investigating the oxidation current of 0.1 mM of L-Trp in pH 7.0 PBS after storage in a refrigerator at 4˚C for one month; the catalytic current response was maintained at 91.3% of its initial value after one month.

The repeatability of the CS/NFCs/GCE was estimated by measuring the current response of 0.1 mM L-Trp for 4 modified electrodes. The relative standard deviation (RSD) was 2.6% ($n = 4$).

3.7. Interference Study

To testify to the selectivity of the sensor, an interference experiment was carried out by recording the electrochemical responses of 0.1 mM Trp on the CS/NFCs/GCE in the electrochemical cell in the presence of potential interfering substances. Several amino acids including leucine, isoleucine, proline, lysine, aspartic acid, valine, and glutamine were used to examine the interference with L-Trp; no significant change in the Trp peak current in the presence of these interfering amino acids was found.

Figure 8 shows the simultaneous detection of Trp with two kinds of important biological substances: ascorbic acid (AA) and uric acid (UA). There were no significant changes in the Trp current peak in the presence of these interfering substances. Based on these results, the CS/NFCs/GCE showed good selectivity for L-Tryptophan determination.

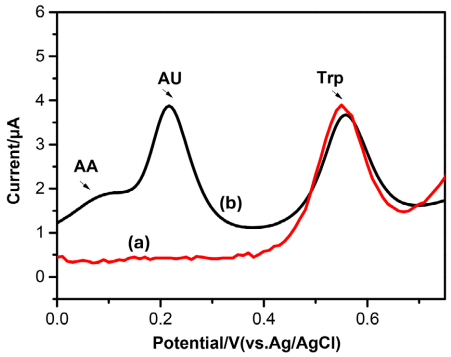

Figure 8. (a) detection of 0.2 mM of L-tryptophan on CS/NFCs/GCE (b) simultaneous detection of 0.2 mM ascorbic acid (AA), 0.1 mM uric acid (UA) and 0.2 mM tryptophan (Trp) on CS/NFC/GCE in 0.01 M phosphate buffer solution (pH 7.0), scan rate 50 mV/s.

3.8. Analysis of Urine Sample

A CS/NFC modified glassy carbon electrode was used to detect Trp in human urine samples. The real samples were collected from healthy volunteer patients with informed consent from the volunteers based on the Declaration of Helsinki. These samples were diluted 100 times with 0.1 phosphate buffer solution (pH7) without any treatment. The standard addition method was applied, so different concentrations of L-Trp were added to the previously diluted human urine. Figure 9 shows the DPV of L-Trp in the concentration range from 8×10^{-3} mM to 12×10^{-3} mM on CS/NFC/GCE, current peaks were observed at 0.55 V.

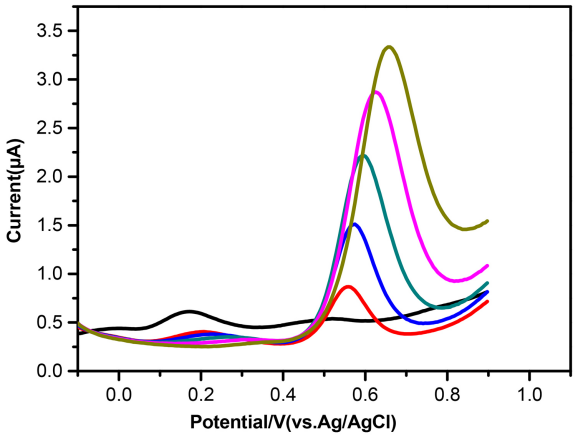

Figure 9. DPV detection of L-tryptophan in human urine sample. Experimental conditions: 0.01 M phosphate buffer solution (pH 7.0), scan rate 50 mV/s.

The equation of the linear relationship between the current and the concentration of L-Trp, in the diluted human urine is: $y = 140.0x + 1.02$. The detected concentration of L-Tryptophan was 7.3×10^{-3} mM (149.1 mg/L). As reported in the literature, the normal range for L-Tryptophan in human urine is 137 - 240 mg/L. The detected value is included in the normal concentration range [40]. Consequently, the obtained results demonstrated that the developed sensing NFC matrix can present a suitable applicability to biological fluids.

4. Conclusion

A stable, sensitive, and selective electrochemical sensor based on nanofibrillated cellulose was successfully developed and applied to the detection of L-Tryptophan. The CS/NFC/GCE exhibited superior electrocatalytic activity and high sensitivity due to the large surface area and conductivity of cellulose nanofibrils. Using the chitosan/nanofibrillated cellulose composite leads to higher detection sensitivity compared to that of synthesized nanomaterials-based sensors. Furthermore, the practical feasibility of the green composite-based sensor for biological fluids was demonstrated in human urine samples. This biosensor could be used for the detection of L-Tryptophan in other biological fluids such as saliva and blood serum.

Acknowledgements

The authors thank the CNRS for financial support through IRP NARES. Campus France is thanked for support through PHC Maghreb EMBISALIM.

Conflicts of Interest

The authors declare no conflicts of interest regarding the publication of this paper.

References

[1] Fiorucci, A.R. and Cavalheiro, É.T.G. (2002) The Use of Carbon Paste Electrode in

the Direct Voltammetric Determination of Tryptophan in Pharmaceutical Formulations. *Journal of Pharmaceutical and Biomedical Analysis*, **28**, 909-915. https://doi.org/10.1016/s0731-7085(01)00711-7

[2] Liu, J., Dong, S., He, Q., Yang, S., Xie, M., Deng, P., *et al.* (2019) Facile Preparation of Fe_3O_4/C Nanocomposite and Its Application for Cost-Effective and Sensitive Detection of Tryptophan. *Biomolecules*, **9**, Article 245. https://doi.org/10.3390/biom9060245

[3] Sundaresan, R., Mariyappan, V., Chen, S., Keerthi, M. and Ramachandran, R. (2021) Electrochemical Sensor for Detection of Tryptophan in the Milk Sample Based on MnWO4 Nanoplates Encapsulated RGO Nanocomposite. *Colloids and Surfaces A*: *Physicochemical and Engineering Aspects*, **625**, Article ID: 126889. https://doi.org/10.1016/j.colsurfa.2021.126889

[4] Sakthivel, R., Mutharani, B., Chen, S., Kubendhiran, S., Chen, T., Al-Hemaid, F.M.A., *et al.* (2018) A Simple and Rapid Electrochemical Determination of L-Tryptophan Based on Functionalized Carbon Black/Poly-L-Histidine Nanocomposite. *Journal of The Electrochemical Society*, **165**, B422-B430. https://doi.org/10.1149/2.0381810jes

[5] Zhang, L., Sun, M., Jing, T., Li, S. and Ma, H. (2022) A Facile Electrochemical Sensor Based on Green Synthesis of Cs/Ce-MOF for Detection of Tryptophan in Human Serum. *Colloids and Surfaces A*: *Physicochemical and Engineering Aspects*, **648**, Article ID: 129225. https://doi.org/10.1016/j.colsurfa.2022.129225

[6] Wang, L., Yang, R., Li, J., Qu, L. and Harrington, P.D.B. (2019) A Highly Selective and Sensitive Electrochemical Sensor for Tryptophan Based on the Excellent Surface Adsorption and Electrochemical Properties of PSS Functionalized Graphene. *Talanta*, **196**, 309-316. https://doi.org/10.1016/j.talanta.2018.12.058

[7] Li, N., Liu, W., Li, W., Li, S., Chen, X., Bi, K., *et al.* (2010) Plasma Metabolic Profiling of Alzheimer's Disease by Liquid Chromatography/Mass Spectrometry. *Clinical Biochemistry*, **43**, 992-997. https://doi.org/10.1016/j.clinbiochem.2010.04.072

[8] Qiu, Y., Cai, G., Su, M., Chen, T., Zheng, X., Xu, Y., *et al.* (2009) Serum Metabolite Profiling of Human Colorectal Cancer Using GC-TOFMS and UPLC-QTOFMS. *Journal of Proteome Research*, **8**, 4844-4850. https://doi.org/10.1021/pr9004162

[9] Yamada, K., Miyazaki, T., Shibata, T., Hara, N. and Tsuchiya, M. (2008) Simultaneous Measurement of Tryptophan and Related Compounds by Liquid Chromatography/Electrospray Ionization Tandem Mass Spectrometry. *Journal of Chromatography B*, **867**, 57-61. https://doi.org/10.1016/j.jchromb.2008.03.010

[10] Alwarthan, A.A. (1995) Chemiluminescent Determination of Tryptophan in a Flow Injection System. *Analytica Chimica Acta*, **317**, 233-237. https://doi.org/10.1016/0003-2670(95)00390-8

[11] Altria, K.D., Harkin, P. and Hindson, M.G. (1996) Quantitative Determination of Tryptophan Enantiomers by Capillary Electrophoresis. *Journal of Chromatography B*: *Biomedical Sciences and Applications*, **686**, 103-110. https://doi.org/10.1016/s0378-4347(96)00037-0

[12] Ren, J., Zhao, M., Wang, J., Cui, C. and Yang, B. (2007) Spectrophotometric Method for Determination of Tryptophan in Protein Hydrolysates. *Food Technology and Biotechnology*, **45**, 360-366.

[13] Gautam, J., Raj, M. and Goyal, R.N. (2020) Determination of Tryptophan at Carbon Nanomaterials Modified Glassy Carbon Sensors: A Comparison. *Journal of the Electrochemical Society*, **167**, Article ID: 066504. https://doi.org/10.1149/1945-7111/ab7e88

[14] Huang, K., Xu, C., Xie, W. and Wang, W. (2009) Electrochemical Behavior and

Voltammetric Determination of Tryptophan Based on 4-Aminobenzoic Acid Polymer Film Modified Glassy Carbon Electrode. *Colloids and Surfaces B*: *Biointerfaces*, **74**, 167-171. https://doi.org/10.1016/j.colsurfb.2009.07.013

[15] Nasimi, H., Madsen, J.S., Zedan, A.H., Malmendal, A., Osther, P.J.S. and Alatraktchi, F.A. (2023) Electrochemical Sensors for Screening of Tyrosine and Tryptophan as Biomarkers for Diseases: A Narrative Review. *Microchemical Journal*, **190**, Article ID: 108737. https://doi.org/10.1016/j.microc.2023.108737

[16] Maciel, J.V., Durigon, A.M.M., Souza, M.M., Quadrado, R.F., Fajardo, A.R. and Dias, D. (2019) Polysaccharides Derived from Natural Sources Applied to the Development of Chemically Modified Electrodes for Environmental Applications: A Review. *Trends in Environmental Analytical Chemistry*, **22**, e00062. https://doi.org/10.1016/j.teac.2019.e00062

[17] Karthik, R., Karikalan, N. and Chen, S. (2017) Rapid Synthesis of Ethyl Cellulose Supported Platinum Nanoparticles for the Non-Enzymatic Determination of H_2O_2. *Carbohydrate Polymers*, **164**, 102-108. https://doi.org/10.1016/j.carbpol.2017.01.077

[18] Zhan, X., Hu, G., Wagberg, T., Zhan, S., Xu, H. and Zhou, P. (2015) Electrochemical Aptasensor for Tetracycline Using a Screen-Printed Carbon Electrode Modified with an Alginate Film Containing Reduced Graphene Oxide and Magnetite (Fe_3O_4) Nanoparticles. *Microchimica Acta*, **183**, 723-729. https://doi.org/10.1007/s00604-015-1718-y

[19] Palanisamy, S., Thangavelu, K., Chen, S., Velusamy, V., Chen, T. and Kannan, R.S. (2017) Preparation and Characterization of a Novel Hybrid Hydrogel Composite of Chitin Stabilized Graphite: Application for Selective and Simultaneous Electrochemical Detection of Dihydroxybenzene Isomers in Water. *Journal of Electroanalytical Chemistry*, **785**, 40-47. https://doi.org/10.1016/j.jelechem.2016.12.019

[20] Zhou, S., Han, X. and Liu, Y. (2016) SWASV Performance toward Heavy Metal Ions Based on a High-Activity and Simple Magnetic Chitosan Sensing Nanomaterials. *Journal of Alloys and Compounds*, **684**, 1-7. https://doi.org/10.1016/j.jallcom.2016.05.152

[21] Bourigua, S., Boussema, F., Bouaazi, D., Mzoughi, Z., Barhoumi, H., Majdoub, H., *et al.* (2024) Sensitive Electrochemical Detection of L-Tryptophan Using a Glassy Carbon Electrode Modified with Pectin Extracted from Arthrocnemum Indicum Leaves. *Journal of Electroanalytical Chemistry*, **953**, Article ID: 117998. https://doi.org/10.1016/j.jelechem.2023.117998

[22] Phanthong, P., Reubroycharoen, P., Hao, X., Xu, G., Abudula, A. and Guan, G. (2018) Nanocellulose: Extraction and Application. *Carbon Resources Conversion*, **1**, 32-43. https://doi.org/10.1016/j.crcon.2018.05.004

[23] Besbes, I., Alila, S. and Boufi, S. (2011) Nanofibrillated Cellulose from TEMPO-Oxidized Eucalyptus Fibres: Effect of the Carboxyl Content. *Carbohydrate Polymers*, **84**, 975-983. https://doi.org/10.1016/j.carbpol.2010.12.052

[24] Jebali, Z., Nabili, A., Majdoub, H. and Boufi, S. (2018) Cellulose Nanofibrils (CNFs) from *Ammophila Arenaria*, a Natural and a Fast Growing Grass Plant. *International Journal of Biological Macromolecules*, **107**, 530-536. https://doi.org/10.1016/j.ijbiomac.2017.09.024

[25] Zinoubi, K., Majdoub, H., Barhoumi, H., Boufi, S. and Jaffrezic-Renault, N. (2017) Determination of Trace Heavy Metal Ions by Anodic Stripping Voltammetry Using Nanofibrillated Cellulose Modified Electrode. *Journal of Electroanalytical Chemistry*, **799**, 70-77. https://doi.org/10.1016/j.jelechem.2017.05.039

[26] Annu, Sharma, S., Nitin, A. and Jain, R. (2020) Cellulose Fabricated Pencil Graphite

Sensor for the Quantification of Hazardous Herbicide Atrazine. *Diamond and Related Materials*, **105**, Article ID: 107788. https://doi.org/10.1016/j.diamond.2020.107788

[27] Velusamy, V., Palanisamy, S., Chen, S., Balu, S., Yang, T.C.K. and Banks, C.E. (2019) Novel Electrochemical Synthesis of Cellulose Microfiber Entrapped Reduced Graphene Oxide: A Sensitive Electrochemical Assay for Detection of Fenitrothion Organophosphorus Pesticide. *Talanta*, **192**, 471-477. https://doi.org/10.1016/j.talanta.2018.09.055

[28] Wang, X., Karaman, C., Zhang, Y. and Xia, C. (2023) Graphene Oxide/Cellulose Nanofibril Composite: A High-Performance Catalyst for the Fabrication of an Electrochemical Sensor for Quantification of P-Nitrophenol, a Hazardous Water Pollutant. *Chemosphere*, **331**, Article ID: 138813. https://doi.org/10.1016/j.chemosphere.2023.138813

[29] Yıldız, C., Eskiköy Bayraktepe, D. and Yazan, Z. (2020) Electrochemical Low-Level Detection of L-Tryptophan in Human Urine Samples: Use of Pencil Graphite Leads as Electrodes for a Fast and Cost-Effective Voltammetric Method. *Monatshefte für Chemie—Chemical Monthly*, **151**, 871-879. https://doi.org/10.1007/s00706-020-02620-7

[30] Zhang, J., Jiang, G., Goledzinowski, M., Comeau, F.J.E., Li, K., Cumberland, T., *et al.* (2017) Green Solid Electrolyte with Cofunctionalized Nanocellulose/Graphene Oxide Interpenetrating Network for Electrochemical Gas Sensors. *Small Methods*, **1**, Article ID: 1700237. https://doi.org/10.1002/smtd.201700237

[31] Laviron, E. (1979) General Expression of the Linear Potential Sweep Voltammogram in the Case of Diffusionless Electrochemical Systems. *Journal of Electroanalytical Chemistry and Interfacial Electrochemistry*, **101**, 19-28. https://doi.org/10.1016/s0022-0728(79)80075-3

[32] Wang, Y., Ouyang, X., Ding, Y., Liu, B., Xu, D. and Liao, L. (2016) An Electrochemical Sensor for Determination of Tryptophan in the Presence of DA Based on Poly(l-Methionine)/graphene Modified Electrode. *RSC Advances*, **6**, 10662-10669. https://doi.org/10.1039/c5ra24116b

[33] Harisha, K.V., Kumara Swamy, B.E. and Ebenso, E.E. (2018) Poly (Glycine) Modified Carbon Paste Electrode for Simultaneous Determination of Catechol and Hydroquinone: A Voltammetric Study. *Journal of Electroanalytical Chemistry*, **823**, 730-736. https://doi.org/10.1016/j.jelechem.2018.07.021

[34] Tasić, Ž.Z., Mihajlović, M.B.P., Radovanović, M.B., Simonović, A.T., Medić, D.V. and Antonijević, M.M. (2022) Electrochemical Determination of L-Tryptophan in Food Samples on Graphite Electrode Prepared from Waste Batteries. *Scientific Reports*, **12**, Article No. 5469. https://doi.org/10.1038/s41598-022-09472-7

[35] Yao, W., Guo, H., Liu, H., Li, Q., Wu, N., Li, L., *et al.* (2020) Highly Electrochemical Performance of Ni-ZIF-8/N S-CNTs/CS Composite for Simultaneous Determination of Dopamine, Uric Acid and L-tryptophan. *Microchemical Journal*, **152**, Article ID: 104357. https://doi.org/10.1016/j.microc.2019.104357

[36] Zhou, S., Deng, Z., Wu, Z., Xie, M., Tian, Y., Wu, Y., *et al.* (2019) Ta_2O_5/rGO Nanocomposite Modified Electrodes for Detection of Tryptophan through Electrochemical Route. *Nanomaterials*, **9**, Article 811. https://doi.org/10.3390/nano9060811

[37] Zagitova, L.R., Maistrenko, V.N., Yarkaeva, Y.A., Zagitov, V.V., Zilberg, R.A., Kovyazin, P.V., *et al.* (2021) Novel Chiral Voltammetric Sensor for Tryptophan Enantiomers Based on 3-Neomenthylindene as Recognition Element. *Journal of Electroanalytical Chemistry*, **880**, Article ID: 114939. https://doi.org/10.1016/j.jelechem.2020.114939

[38] You, H., Mu, Z., Zhao, M., Zhou, J., Chen, Y. and Bai, L. (2018) Voltammetric Aptasensor for Sulfadimethoxine Using a Nanohybrid Composed of Multifunctional Fullerene, Reduced Graphene Oxide and Pt@Au Nanoparticles, and Based on Direct Electron Transfer to the Active Site of Glucose Oxidase. *Microchimica Acta*, **186**, Article 1. https://doi.org/10.1007/s00604-018-3127-5

[39] Karim-Nezhad, G., Sarkary, A., Khorablou, Z. and Seyed Dorraji, P. (2018) Electrochemical Analysis of Tryptophan Using a Nanostructuring Electrode with Multi-Walled Carbon Nanotubes and Cetyltrimethylammonium Bromide Nanocomposite. *Journal of Nanostructures*, **8**, 266-275.

[40] Berg, C.P. and Rohse, W.G. (1947) The Tryptophan Content of Normal Human Urine. *Journal of Biological Chemistry*, **170**, 725-729. https://doi.org/10.1016/s0021-9258(17)30854-2